Photodiagnosis and Photodynamic Therapy 34 (2021) 102290

Contents lists available at ScienceDirect

Photodiagnosis and Photodynamic Therapy

journal homepage: www.elsevier.com/locate/pdpdt

Photo-genosensor for *Trichomonas vaginalis* based on gold nanoparticles-genomic DNA

S. Ilbeigi [a], R. Dehdari Vais [a], N. Sattarahmady [a,b,*]

[a] Nanomedicine and Nanobiology Research Center, Shiraz University of Medical Sciences, Shiraz, Iran
[b] Department of Medical Physics, School of Medicine, Shiraz University of Medical Sciences, Shiraz, Iran

ARTICLE INFO

Keywords:
T. vaginalis
Trichomoniasis
Visual detection
Au nanoparticles
DNA biosensor

ABSTRACT

Trichomoniasis, an infectious disease caused by a parasite called *Trichomonas vaginalis* (*T. vaginalis*), enhances the risk of HIV infection, cervical and prostate cancer, and infertility. Therefore, efforts have to be made for accurate, specific, and rapid diagnosise and treatment of trichomoniasis. Today, optical nanosensors have created an opportunity for diagnosis without sophisticated and expensive tools and the need for expertise; at the same time, they are highly sensitive and fast.

An optical nano-genosensor was designed by conjugation of gold nanoparticles and a specific oligonucleotide (AuNPs-probe) from repeated DNA target for specific and sensitive polymerase chain reaction diagnosis of *T. vaginalis* gene sequence (L23861.1). The hybridization of AuNPs-probe was investigated with different concentrations of complementary sequence in synthesized target, gene sequence of standard *T. vaginalis* genomic DNA extraction, and PCR products of genomic DNA samples extracted from patients. Negative samples including synthesized non-complementary sequence, genomics DNA of other pathogens, and genomics DNA of healthy persons were considered for proof of the accuracy of the sensor function. The occurrence of correct hybridization was detected by adding acid to the medium and observing the changes in the color of the medium and spectroscopic spectrum. Based on spectrophotometric results, the fabricated genosensor had detection limits of 35.16 and 31 pg μL^{-1} for the detection of synthetic target and genomic DNA sequences, respectively. The results confirmed the correct function of genosensor for the detection of *T. vaginalis* in clinical samples. Advantages such as low cost, visual detection, speed, and easy diagnosis encourage the use of this sensor in pathogen detection in the future.

1. Introduction

Trichomonas vaginalis (*T. vaginalis*), a flagellated protozoan which results in Trichomoniasis, is the most common form of non-viral infection among women with about 276.4 million cases worldwide [1,2]. *T. vaginalis* resides in the vagina and urethra of the females, and the urethra and prostate of the males. As we know, humans are the only known host for *T. vaginalis*, and transmission occurs among sexual contact [3,4]. *T. vaginalis* is an extracellular pathogen that adheres to the epithelial host cells, colonizes, and establishes the infection [5]; it causes asymptomatic infection in males and a series of symptoms including cervicitis and vaginitis in women [6]. Several cross-sectional studies have also shown that *T. vaginalis* increases the risk of HIV infection [7]. The fact that *T. vaginalis* is associated with more serious diseases like cervical cancer in women and prostate cancer in men and infertility [8] necessitates more efforts to accurately diagnose and treat trichomoniasis.

In recent years, different methods have been used for detection of trichomoniasis, such as wet mount microscopy, culture, ELISA, immunofluorescence, PCR etc. [9] (see also Table 1). Wet mount microscopy is a low cost and poor technology method with low sensitivity and has been used for many years [10,11], while the sensitivity of the culture method is high; it takes a long time and needs high-quality specimens and a professional microscopic examiner [12]. *T. vaginalis* can be evaluated with ELISA and immunofluorescence tests; the later test has shown a sensitivity and specificity of 88 % and 99 %, respectively [13]. The ELISA test needs expensive antibodies and has a long detection time [6]. Although PCR-based assays have a high sensitivity and specificity, with an accuracy of 10–31 copies per reaction, they need expensive instruments, direct detection of PCR products are impossible, and PCR

* Corresponding author at: Nanomedicine and Nanobiology Research Center, Shiraz University of Medical Sciences, Shiraz, Iran.
E-mail addresses: nsattar@sums.ac.ir, sattarahmady@yahoo.com (N. Sattarahmady).

https://doi.org/10.1016/j.pdpdt.2021.102290
Received 5 December 2020; Received in revised form 20 March 2021; Accepted 5 April 2021
Available online 8 April 2021

Table 1
Comparison between different reported methods for *T. vaginalis* detection.

Detection method	LOD	Reference
Real-time PCR	10 copies per reaction	[42]
Real-time PCR	40 copies/mL	[43]
Real-time PCR	<0.2 organism per reaction	[44]
Real-time PCR-fluorescence resonance energy transfer	1.06 organism	[45]
Real-time PCR melting curve	<200 copies/μL	[46]
PCR	7−31 copies per reaction	[47]
PCR	0.021 copies	[48]
Loop-mediated isothermal amplification	0.036 ng/μL	[18]
Loop-mediated isothermal amplification	1 pg per reaction	[19]
Lateral flow immunoassay	7 genome equivalents/mL	[49]
MALDI-TOF MS[1]	10^5 trophozoites/mL	[20]
Au-NP probe hybridization assay-Target DNA-Spectrophotometry	23 pg/μL	Present study
Au-NP probe hybridization assay-Target DNA-Visual	2.5 ng, 0.1 ng/μL (LOQ)	Present study
Au-NP probe hybridization assay for genomic DNA	31 pg/μL	Present study

products need to be analyzed by gel electrophoresis [14–17]. Loop-mediated isothermal amplification (LAMP) that involves amplification of target DNA by DNA polymerase is another method for detection of *T. vaginalis*. The LAMP technique is as equally sensitive and specific as qPCR method [18]. Although this method is highly sensitive with a detection limits of 1 trichomonad and 1 pg of *T. vaginalis* DNA per reaction, it still needs DNA electrophoresis to asset ladder-pattern in DNA electrophorese or recognition by fluorescent detection dyes, such as SYBR green [19]. Another technique of *T. vaginalis* detection is Lateral flow immunoassay with a detection limit (LOD) of 7 genomic DNA per mL of a sample [20]. In spite of the fact that this method provides quantitative results, it required special equipments and softwares (scanners, reflectometers and CCD camera) [21]. Therefore, there is a need for a rapid, low-cost and direct detection method with acceptable sensitivity and specificity for the detection of *T. vaginalis*.

Due to their unique properties, nanoscale materials play impressive roles in various fields of biology including biologicals delivery, pathogen and disease detection, disease treatment and detection [22–28]. Recent improvement in nanotechnology has provided new and precise techniques for detection of different pathogens, biomolecules, drugs and chemicals [16,17,29–32]. Metallic nanomaterials with specific physicochemical properties including optical and electronic behaviors have been recently opened accurate, rapid and highly sensitive routes for biomolecular and medical diagnosis [15,16,24,28,30,32–35]. For example, coherent free electrons in the conduction band of gold nanoparticles (AuNPs) induce surface plasmon resonance. The range of the plasmon band in UV–vis spectra is strongly influenced by the size and modification of AuNPs surface and also its environment physicochemical properties [24]. Plasma band tracking of AuNPs by monitoring the changes in the color of the medium and UV–vis spectra provides an opportunity for use in diagnostic testing [33,36,37].

Conjugation of DNA with nanomaterials as AuNPs-probes is an efficient nano- biosensing principal [38]. Hill and Mirkin in 1996 were the first ones to use oligonucleotide probes that were conjugated with AuNPs for detection of DNA [33]. AuNPs are very efficient biosensor transducer due to their special properties; the ability to easily conjugation with a variety of biomolecules, large surface area, surface-enhanced Raman scattering (SERS) and Rayleigh resonance scattering (RRS), make them a system for detection of biomolecules [33,36,37]. AuNPs-probe hybridization with a target DNA sequence and change in the conditions of reagent medium such as pH or ionic strength induce color change and made it visually real-time detectable just with naked eyes [39–41].

This study aimed to design an AuNPs-probe biosensor based on DNA sequences for simple and powerful detection of *T. vaginalis* with high sensitivity and specificity, and evaluate the pathogen both visually and spectrophotometrically.

2. Experimental section

2.1. Materials and tools

Standard strains of *Enterococcus* faecalis (*E. faecalis*, PTCC 1237), *Escherichia coli* (*E. coli*, PTCC 1399), and *Staphylococcus aureus* (*S. aureus*, PTCC 1431) species were purchased from Iranian Organization of Science and Technology (Iran). Chloroauric acid and tri-sodium citrate were purchased from Sigma (USA). A thiolated oligonucleotide probe was designed (vide infra) and prepared from Bioneer Co. (Korea). PCR primers used in this study were selected based on the sequence of *T. vaginalis* [41], and purchased from Sinaclon Co. (Iran). A genomic DNA extraction kit was purchased from CinnaGen (Iran). All other chemicals were purchased from Merck (Germany).

2.2. Genomic DNA extraction

A common *T. vaginalis* isoform (*T. vaginalis* G3 assembly ASM282v1) isolated from the cases in the south of Iran was obtained. *T. vaginalis* was recovered from frozen samples, grown and maintained at 37 °C in TYI-S-33 medium containing 10 % heat-inactivated adult bovine serum (Sigma), 1 % pen-strep (Sigma), and 2 % multivitamin mixture (Biofluids Inc. Rockville). The medium was refreshed every 2–3 days and the culture was split before reaching a density of 1×10^6 cell mL^{-1}. The cells were used after ten subcultures. DNA was extracted from *T. vaginalis* culture using a genomic DNA extraction kit (DNA Bio TM, Iran) according to the manufacturer's instruction, and stored at -20 °C until use. The concentration of genomic DNA was determined using a Thermo Scientific NanoDrop 2000c (USA).

DNA samples were extracted from the cultures of *E. faecalis*, *E. coli* and *S. aureus*. DNA extraction was performed using the DNP™ genomic DNA kit and stored at −20 °C until use. The amount of genomic DNA was determined using a Thermo Scientific NanoDrop 2000c (USA).

2.3. Clinical samples

Swab samples of vaginal discharges were taken from patients with trichomoniasis admitted to a hospital in sterile conditions. Then, the vaginal discharge swabs were immersed in 500 μL of a 100 mmol L^{-1} phosphate buffer saline (PBS) solution (pH 7.4) for 30 min. Then, the genomic DNA of the samples was extracted by a DNA extraction kit (DNA Bio TM, Iran), according to the manufacturer's instruction. The amplification of the extracted genomic DNA was conducted using PCR. PCR was carried out using *T. vaginalis* specific primers and a PCR purification kit (Takara, Japan), according to the manufacturer's instruction. The thermal cycling condition was set as follows: 95 °C for 5 min followed by 35 cycles of 95 °C for 45 s, annealing at 55 °C for 45 s, extension at 72 °C for 40 s, and final step at 72 °C for 5 min, and finally, held at 4 °C until use. The concentration of amplified DNA samples was then determined using a NanoDrop spectrophotometer followed by gel electrophoresis to ensure PCR product bands.

2.4. Preparation of AuNPs

AuNPs were synthesized by the citrate reduction route, as previously reported [33,38]. Briefly, sodium citrate (25 mL, 38.8 mmol L^{-1}) was added into a heated chloroauric acid solution (250 mL, 1 mmol L^{-1}), and the mixture was refluxed for 15 min. The obtained AuNPs solution had a peak in UV–vis spectra using a UV–vis spectrophotometer of Rayleigh 2100 (China), with a maximum peak at 520 nm, confirming the

appropriate size and size distribution of the nanoparticles. Then, the AuNPs solution was stored in a cool and dark place. The size and morphology of AuNPs were also determined by transmission electron microscopy (TEM) using a Zeiss, EM10C microscope (Germany).

2.5. Oligonucleotide (probe) design

A 24-base thiolated oligonucleotide (5'-HS $(CH_2)_6$TTTTTTTTTTGAAGTCCTTCGGTTC-3') was designed using NCBI BLAST nucleotide search tool and Primer3 based on the submitted sequence in GenBank for *T. vaginalis*. The probe sequence was checked for any possible homology and share sequences with any non-*T. vaginalis* species. Moreover, the melting temperature of the probe was ensured to be within a narrow range using Oligo software. Then, the probe sequence was checked for potential self-dimer and formation of secondary structures using mfold software (http://mfold.rna.albany.edu) which may otherwise hinder the assay.

2.6. Preparation of AuNPs-probe

The probe was firstly suspended into a dithiothreitol (DTT) solution (0.1 mmol L^{-1}, pH 8.3) at room temperature for 60 min, to ensure complete disulfide cleavage for reaction of the -SH group with AuNPs. Then, the mixture was centrifuged for washing, and ethanol precipitation was done. This was repeated three times.

The AuNPs-probe was prepared as previously reported [33]. Shortly, 82.8 pmol of the DTT-treated probe solution was mixed with the AuNPs solution to a volume of 1000 µL, and the mixture was shaken for 16 h overnight in dark. Then, PBS (pH 7.0) containing sodium dodecyl sulfate (0.1 %) was added to this solution, to obtain a final concentration of 10 mmol L^{-1}. After 48 h, sodium chloride was continuously added to a final concentration of 0.1 mol L^{-1}, centrifuged, and re-suspended in PBS (pH 7.0) for AuNPs-probe separation. The solution was stored in dark at 4 °C until use. This AuNPs-probe had the same red color as AuNPs with no visible aggregates.

2.7. AuNPs-probe hybridization assays

To ensure the best observation of color changes and optimize the conditions of hybridization, we mixed various amounts of HCl and deionized water in different ratios with various amounts of AuNP-probe to attain the best color changes. Different amounts of the target DNA (5'-GAACTTTAACCGAAGGACTTC-3', 2.5, 3.2, 4.8, 5.1, 12.8, 19.2, 25.6, 32.0, 38.4, 44.8 and 51.2 ng), which was a complement of the probe sequence, dissolved in 10 mmol L^{-1} PBS (pH 5.0), were reached the final volume of 10 µL, and then were heated to 95 °C for 5 min in a closed-cap microtube. 15 µL of the AuNP-probe was added to each diluted target DNA solution and immediately incubated at 65 °C for 12 min. Also, a sample was prepared in the same protocol using 12.8 ng of a non-complementary sequence as non-target DNA to the final volume of 10 µL. After addition of 4 µL HCl 0.5 mol L^{-1}, the absorbance of the solutions was measured spectrophotometrically, and also the color of the solutions was recorded by a camera.

To determine the limits of detection and quantitation (LOQ) of genomic DNA using AuNP-probe, we applied the hybridization assay to *T. vaginalis* genomic DNA. 10 µL of the genomic DNA of *T. vaginalis* samples (0.3, 0.6, 1.2, 2.5, 5.0, 10, 20, 26 and 32 ng) were evaluated with the AuNP-probe. Blank control samples including 10 mmol L^{-1} PBS (pH 5.0) without genomic DNA were evaluated. Also, 30 ng genomic DNA of *E. coli*, *E. faecalis* and *S. aureus* was used as negative controls. A sample containing 10 µL of a mixture of genomic DNA of *T. vaginalis*, *E. coli* and *E. faecalis* in ratios of 3:1:1 was evaluated with the AuNP-probe. The above solutions were incubated at 95 °C for 5 min followed by incubation at 65 °C for 12 min. Subsequently, the solutions were subjected to acid addition and then evaluated both visually and spectrophotometrically.

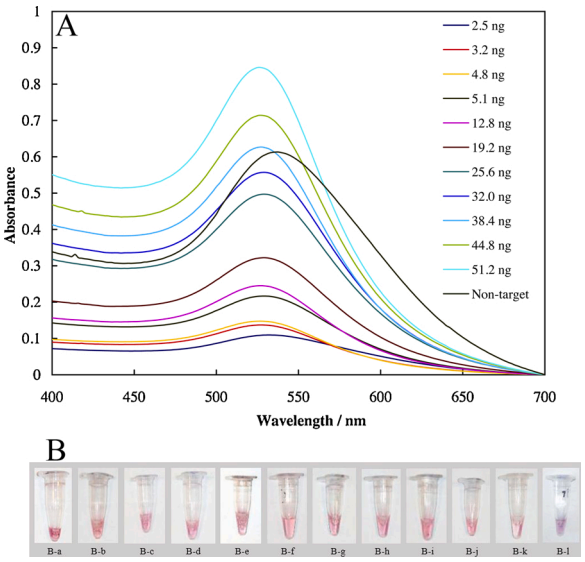

Fig. 1. UV–vis spectra (A) and visual color changes (B) after addition of 4 µL HCl (0.5 mol L^{-1}) to the AuNPs-probe solution hybridized in the presence of different concentrations of the target sequence of 2.5 (B-a), 3.2 (B-b), 4.8 (B-c), 5.1 (B-d), 12.8 (B-e), 19.2 (B-f), 25.6 (B-g), 32.0 (B-h), 38.4 ng (B-i), 44.8 ng (B-j), 51.2 ng (B-k), or 12.8 ng (B-l) non-target sequence in PBS, pH 5.0.

2.8. Colorimetric detection of clinical samples

For hybridization assay, 5 µL of 10 mmol L^{-1} PBS (pH 5.0) and 10 µL of the extracted genomic DNA from *T. vaginalis* clinical samples of two patients and two negative controls (healthy individuals) were heated at 95 °C for 10 min. Then, 15 µL of AuNPs-probe was added and incubated at 65 °C for 12 min. 3 µL 0.5 mmol L^{-1} HCl was then added and the results were evaluated visually and spectrophotometrically. Before these stages, PCR amplification for all clinical samples was done.

3. Results and discussion

3.1. Characterization and probe conjugation into AuNPs

A TEM image and a UV–vis spectrum of the synthesized AuNPs are presented in supplementary material (S1). AuNPs solution with a pink color presented a maximum absorbance of 524 nm, narrow size distribution, and spherical shape of about 16 ± 3 nm (n = 50) in diameter. The probe was designed from the submitted nucleotide sequence of *T. vaginalis* in GenBank with access number of L23861.1. The stability and durability of the AuNPs-probe solution were followed for three months without any aggregation, absorbance maximum change, or color change observation.

3.2. Detection of the target sequence

Hybridization test was carried out for various amounts of the target sequence (2.5–51.2 ng) as well as non-target ones (12.8 ng) to assess and optimize the ability of AuNPs-probe to hybridize with the target sequence and its differentiation from the others. Fig. 1 presents UV–vis spectra (A) and visual colors (B) of the AuNPs-probe solution in the presence of various amounts of the target or non-target sequences following acid addition. Existence of the target sequence in the AuNPs-probe solution led to hybridization and formation of double-stranded DNA; it stabilized AuNPs against aggregation through acid addition. In another way, AuNPs-probe became clustered and aggregated following acid addition in non-hybridization situations. In the presence of the non-target sequence, there was a ~10 nm shift in UV–vis spectra in the absorption maximum, and the solution color became purple. This resulted

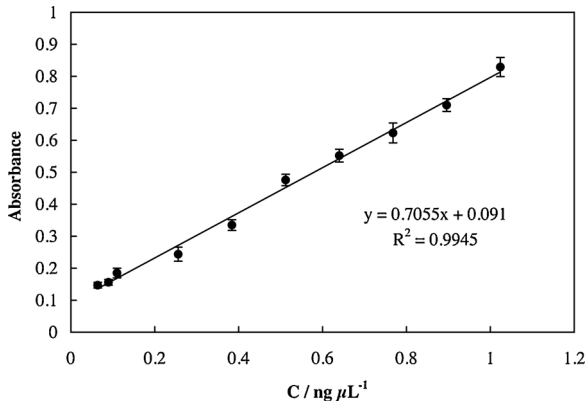

Fig. 2. A calibration plot for the spectrophotometric determination of *T. vaginalis* target sequence by the AuNPs-probe hybridization assay.

from the instability of AuNPs and aggregate formation after acid addition. While, AuNPs-probe hybridization with the target sequence led to a stable double-strand structure which prevents AuNPs from aggregation following acid addition. Visually, presence of the target sequence was detected by becoming pink-red color of the AuNPs solution.

Spectrophotometrically, the concentration of the target sequence in the solution determined the intensity of maximum absorbance. A wide peak in the spectrum with a maximum absorbance of 530 nm was observed for 2.5 ng target sequence, which determines the outer range of limit detection of designed AuNPs-probe. Higher concentrations of the target sequence represented a peak in the spectra upon acid addition with blue shifts for the absorbance maxima.

Color of the AuNPs-probe solution also returned to purple in the presence of 2.5 ng target sequence, upon acid addition. Therefore, 2.5 ng of the target sequence was the lowest amount of the target to form adequate amounts of double strands around the AuNPs surface to avoid aggregation following acid addition. This value, that was equal to a concentration of 0.1 ng μL^{-1}, was considered as the visual LOQ of the target sequence.

Fig. 2 represents a calibration curve for the spectrophotometric determination of the target sequence upon hybridization with AuNPs-probe and after acid addition. The calibration curve represented a regression equation of $y = 0.7055x+0.091$, with $R^2 = 0.9945$ in a linear range of 0.06–1.02 ng μL^{-1}. LOD of the assay was also obtained as 23 pg μL^{-1}, based on 3SD/b criterion (SD and b are the standard deviation of the blank signal and the slope of the calibration curve, respectively).

3.3. Application of AuNPs-probe for genomic DNA determination

AuNPs-probe hybridization assay for genomic DNA determination was done on DNA extracts of the standard cultures of *T. vaginalis*. Fig. 3A represents spectrophotometric spectra of AuNPs-probe upon hybridization with different concentrations of *T. vaginalis* genomic DNA (0.3, 0.6, 1.2, 2.5, 5.0, 10, 20, 26 and 32 ng) after acid addition. A maximum absorption peak at 530 nm was observed for different concentrations of *T. vaginalis* genomic DNA. The maximum absorbance values depended on the amount and concentration of genomic DNA. Using the spectra, a calibration curve for the *T. vaginalis* genomic DNA and AuNPs-probe hybridization can be plotted, and is shown in Fig. 3B. The calibration plot represented a linear dependency of the absorbance on the concentration with a regression equation of $y = 0.8008x+0.2389$, with $R^2 = 0.9851$ in linear range of 0.0034 to 0.32 ng μL^{-1}. It can also resulted in a value of 31 pg μL^{-1} as LOD of the spectrophotometric detection of *T. vaginalis* genomic DNA.

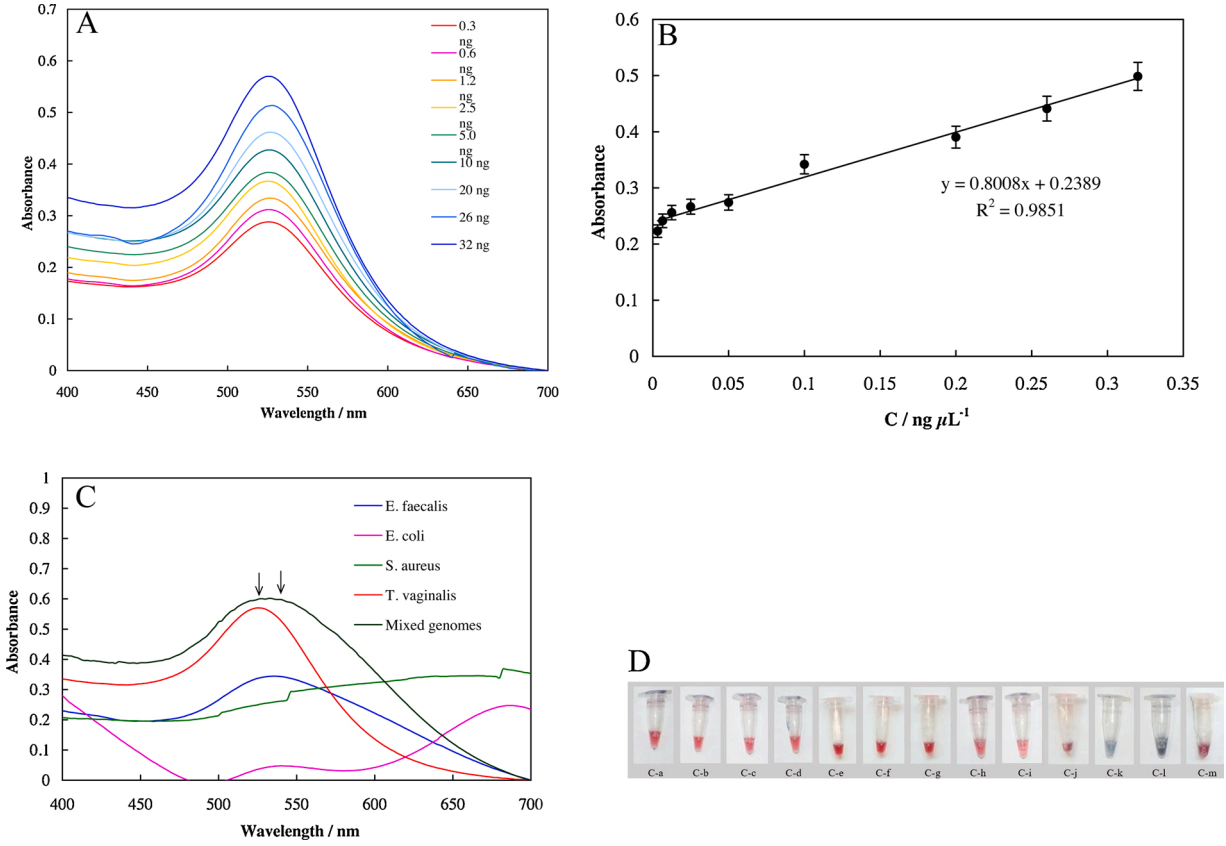

Fig. 3. UV–vis spectra (A, C) and visual images (D) of different amounts of *T. vaginalis* genomic DNA of 0.3 (D-a), 0.6 (D-b), 1.2 (D-c), 2.5 (D-d), 5.0 (D-e), 10 (D-f), 20 (D-g), 26 (D-h), 32 (D-i) and 40 ng (D-j), and 30 ng of *E. coli* (D-k), *S. aureus* (D-l) and *E. faecalis* genomic DNA (D-m). (B) A calibration plot for the spectrophotometric determination of *T. vaginalis* genomic DNA.

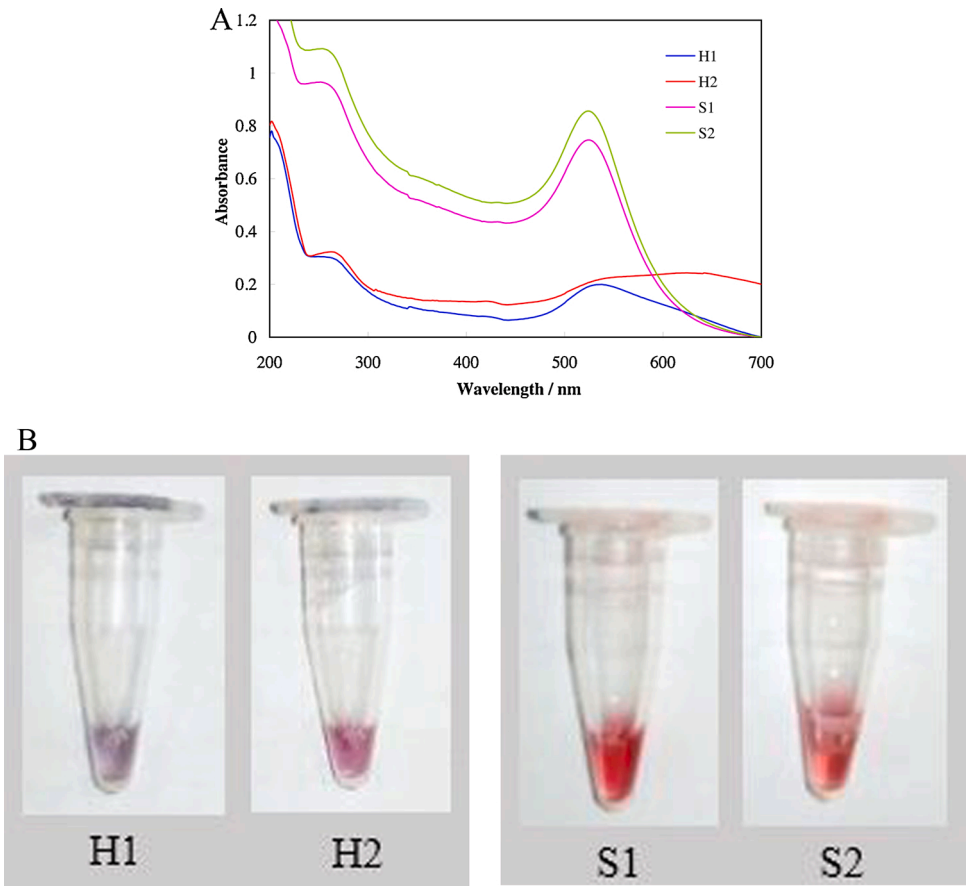

Fig. 4. UV–vis spectra (A) and visual images (B) of PCR products of extracted DNA from clinical samples of trichomoniasis patients (S1, S2) and healthy persons (H1, H2), after AuNPs-probe hybridization assay.

Fig. 3C shows spectrophotometric spectra of AuNPs-probe upon hybridization with genomic DNA of *E. coli* (30 ng), *S. aureus* (30 ng), *E. faecalis* (30 ng) and a mixture of *T. vaginalis*, *E. coli* and *E. faecalis* (3:1:1) genomes after acid addition. Genomic DNA of standard species of *E. faecalis*, *E. coli*, and *S. aureus* were tested as negative samples. While for different concentrations of *T. vaginalis* genomic DNA an absorption peak at 530 nm was observed, the maximum absorption of UV–vis spectra of *E. coli*, *S. aureus*, and *E. faecalis* genomic DNA samples had red shifts without any definite maximum absorbance. The most similarity between the spectra of the negative samples with that of *T. vaginalis* genomic DNA was for *E. faecalis* genomic DNA. However, it seems that the absorption maxima had enough difference to resolve *T. vaginalis* from *E. faecalis* genomic DNA. On the other hand, the more yellowish absorption also seems to be enough for the complementary light to be purple (instead of the red for *T. vaginalis*, vide infra). In addition, the absorption pattern of the spectra for the mixture of *T. vaginalis*, *E. coli* and *E. faecalis* genomic DNA showed the presence of both *T. vaginalis* and *E. faecalis* genomic DNA with distinguishable absorption maxima (indicated by arrows in Fig. 3C). The data indicated quantitation of *T. vaginalis* in the presence of the other pathogens, and the selectivity performance of the AuNPs-probe to capture the *T. vaginalis* genomic DNA.

Fig. 3D shows the colors of AuNPs-probe solutions in the presence of different concentrations of *T. vaginalis* genomic DNA, and one concentration of *E. coli*, *S. aureus* and *E. faecalis* genomic DNA, upon acid addition. In the images, red color of the AuNPs-probe stayed after hybridization with the *T. vaginalis* genome, even in the presence of 0.3 ng of *T. vaginalis*. However, purple colors were visualized after acid addition in the samples containing genomic DNA of *E. coli*, *S. aureus* and *E. faecalis*. These results confirmed the ability of the AuNPs-probe for visual detection and selection of the *T. vaginalis* genomic DNA.

3.4. Analysis of clinical samples

Validation of the synthesized AuNPs-probe was analyzed for PCR product of the extracted genomic DNA from two suspicious *T. vaginalis* infected patients (S1 and S2) and two healthy ones (H1, H2). Fig. 4A shows UV–vis spectra of these clinical samples which tolerated AuNPs-probe hybridization assay and acid addition. In the spectra, S1 and S2 samples represented maximum absorbances at 522 nm, while the spectra of H1 and H2 samples were wide with no clear maximum absorbance. Fig. 4B shows visual photographic images of these samples (patients and healthy individuals) after the AuNP-probe hybridization assay and acid addition. The color of S1 and S2 (patient samples) remained red, while those of H1 and H2 (healthy individuals) turned to purple. The accuracy of the AuNPs-probe and hybridization test performance for clinical samples was consistent with the PCR results of these samples. For the detection of clinical samples, low cost, fast reading of the results and visual detection with the naked eye are the advantages. A comparison between different reported methods for *T. vaginalis* detection is presented in Table 1 indicating deservingness of the assays presented in this research. Visual detection not only do not need sophisticated and expensive instruments, are highly sensitive and fast, have a wide dynamic range, and are easy-to-use in comparison with other methods.

4. Conclusion

In this study, a specific oligonucleotide conserved sequence of *T. vaginalis* was selected as a specific diagnosis probe, and an optical

sensing route was programmed based on the AuNPs-conjugated probe. Hybridization experiments with AuNPs-probe were performed for serial dilutions of the synthesized complementary sequence, gene sequence of the standard *T. vaginalis* genomic DNA extracts and PCR products of genomic DNA samples extracted from patients. The outcomes of the hybridization test were analyzed based on visual and spectroscopic detections. The results indicated valuable sensitivity and specificity of the proposed AuNPs-probe for the diagnosis of *T. vaginalis*, whose repeatability, stability and economic efficiency make it useful for clinical diagnosis applications.

Acknowledgment

We would like to thank the Research Council of Shiraz University of Medical Sciences (23439) with ethical code of 891 for supporting this research.

Appendix A. Supplementary data

Supplementary material related to this article can be found, in the online version, at doi:https://doi.org/10.1016/j.pdpdt.2021.102290.

References

[1] A.E. Wiringa, R.B. Ness, T. Darville, R.H. Beigi, C.L. Haggerty, Trichomonas vaginalis, endometritis and sequelae among women with clinically suspected pelvic inflammatory disease, Sex. Transm. Infect. 96 (2020) 436–438.
[2] O.T. Van Gerwen, C.A. Muzny, Recent advances in the epidemiology, diagnosis, and management of Trichomonas vaginalis infection, F1000Research 8 (2019). F1000 Faculty Rev-1666.
[3] D.F. Harp, I. Chowdhury, Trichomoniasis: evaluation to execution, Eur. J. Obstet. Gynecol. Reprod. Biol. 157 (2011) 3–9.
[4] P. Kissinger, Trichomonas vaginalis: a review of epidemiologic, clinical and treatment issues, BMC Infect. Dis. 15 (2015) 1–8.
[5] Y.R. Nievas, V.M. Coceres, V. Midlej, W. de Souza, M. Benchimol, A. Pereira-Neves, A.A. Vashisht, J.A. Wohlschlegel, P.J. Johnson, N. de Miguel, Membrane-shed vesicles from the parasite Trichomonas vaginalis: characterization and their association with cell interaction, Cell. Mol. Life Sci. 75 (2018) 2211–2226.
[6] T. Edwards, P. Burke, H. Smalley, G. Hobbs, Trichomonas vaginalis: clinical relevance, pathogenicity and diagnosis, Crit. Rev. Microbiol. 42 (2016) 406–417.
[7] P. Kissinger, A. Adamski, Trichomoniasis and HIV interactions: a review, Sex. Transm. Infect. 89 (2013) 426–433.
[8] S.H. Tsang, S.F. Peisch, B. Rowan, S.C. Markt, A.G. Gonzalez-Feliciano, S. Sutcliffe, E.A. Platz, L.A. Mucci, E.M. Ebot, Association between Trichomonas vaginalis and prostate cancer mortality, Int. J. Cancer 144 (2019) 2377–2380.
[9] C. Adjei, R. Boateng, A. Dompreh, B. Okyere, E.-W. Owiredu, Prevalence and the evaluation of culture, wet mount, and ELISA methods for the diagnosis of Trichomonas vaginalis infection among Ghanaian women using urine and vaginal specimens, Trop. Med. Health 47 (2019) 33.
[10] M.A. Kingston, D. Bansal, E.M. Carlin, 'Shelf life' of Trichomonas vaginalis, Int. J. STD AIDS 14 (2003) 28–29.
[11] S. Nabweyambo, O. Kakaire, S. Sowinski, A. Okeng, H. Ojiambo, J. Kimeze, I. Najjingo, F. Bwanga, Very low sensitivity of wet mount microscopy compared to PCR against culture in the diagnosis of vaginal trichomoniasis in uganda: a cross-sectional study, BMC Res. Notes 10 (2017) 1–6.
[12] Y. Li, S. Wang, H. Li, X. Song, H. Zhang, Y. Duan, C. Luo, B. Wang, S. Ji, Q. Xie, Z. Zhang, Development of a convenient detection method for Trichomonas vaginalis based on loop-mediated isothermal amplification targeting adhesion protein 65, BMC Infect. Dis. 20 (2020) 1–8.
[13] Y. Tian, C. Xiong, H. Guan, X. Pang, C. Jiang, Detection of Trichomonas vaginalis with direct immunofluorescence assay, Chin. J. Parasitol. Parasitic Dis. 21 (2003) 242–244.
[14] C.S. Noh, S.S. Kim, S.Y. Park, H.S. Moon, Y. Hong, J.S. Ryu, Comparison of two PCR assays for Trichomonas vaginalis, Korean J. Parasitol. 57 (2019) 27.
[15] R. Nazari-Vanani, N. Sattarahmady, H. Yadegari, M. Khatami, H. Heli, Electrochemical biosensing of 16s rRNA gene sequence of Enterococcus Faecalis, Biosens. Bioelectron. 142 (2019), 111541.
[16] R. Nazari-Vanani, N. Sattarahmady, H. Yadegari, H. Heli, A novel and ultrasensitive electrochemical DNA biosensor based on anice crystals-like gold nanostructure for the detection of Enterococcusfaecalis gene sequence, Colloids Surf. B Biointerfaces 166 (2018) 245–253.
[17] R. Nazari-Vanani, H. Heli, N. Sattarahmady, An impedimetric genosensor for Leishmania infantum based on electrodeposited cadmium sulfide nanosheets, Talanta 217 (2020), 121080.
[18] R. Martzy, C. Kolm, K. Brunner, R.L. Mach, R. Krska, H. Sinkovec, R. Sommer, A. H. Farnleitner, G.H. Reischer, A loop-mediated isothermal amplification (LAMP) assay for the rapid detection of Enterococcus spp. in water, Water Res. 122 (2017) 62–69.
[19] Y.K. Goo, W.S. Shin, H.W. Yang, S.Y. Joo, S.M. Song, J.S. Ryu, H.H. Kong, W.K. Lee, D.I. Chung, Y. Hong, Loop-mediated isothermal amplification targeting actin DNA of Trichomonas vaginalis, Korean J. Parasitol. 54 (2016) 329–334.
[20] A. Calderaro, M. Piergianni, S. Montecchini, M. Buttrini, G. Piccolo, S. Rossi, M. C. Arcangeletti, M.C. Medici, C. Chezzi, F. De Conto, MALDI-TOF mass spectrometry as a potential tool for Trichomonas vaginalis identification, BMC Infect. Dis. 16 (2016) 261.
[21] B.G. Andryukov, Six decades of lateral flow immunoassay: from determining metabolic markers to diagnosing COVID-19, AIMS Microbiol. 6 (2020) 280–304.
[22] Z. Yazdani, H. Yadegari, H. Heli, A molecularly imprinted electrochemical nano biosensor for prostate-specific antigen determination, Anal. Biochem. 566 (2019) 116–125.
[23] M. Khatami, H. Heli, P.M. Jahani, H. Azizi, M.A.L. Nobre, Copper/copper oxide nanoparticles synthesis using stachys lavandulifolia and its antibacterial activity, IET Nanobiotechnol. 11 (2017) 709–713.
[24] H. Heli, A. Rahi, Synthesis and applications of nanoflowers, Recent Pat. Nanotechnol. 10 (2016) 86–115.
[25] M. Tabeshnia, H. Heli, A. Jabbari, A.A. Moosavi-Movahedi, Electrooxidation of some non-steroidal anti-inflammatory drugs on an alumina nanoparticle-modified glassy carbon electrode, Turk. J. Chem. 34 (2010) 35–46.
[26] N. Sattarahmady, M. Heidari, T. Zare, M. Lotfi, H. Heli, Zinc-nickel ferrite nanoparticles as a contrast agent in magnetic resonance imaging, Appl. Magn. Reson. 47 (2016) 925–935.
[27] H. Heli, J. Pishahang, H. Barzegar Amiri, Synthesis of hexagonal CoAl-layered double hydroxide nanoshales/carbon nanotubes composite for the non-enzymatic detection of hydrogen peroxide, J. Electroanal. Chem. 768 (2016) 134–144.
[28] R. Dehdari Vais, N. Sattarahmady, K. Karimian, H. Heli, Green electrodeposition of gold hierarchical dendrites of pyramidalnanoparticles and determination of azathioprine, Sens. Actuators B 215 (2015) 113–118.
[29] N.C. Tansil, Z. Gao, Nanoparticles in biomolecular detection, Nano Today 1 (2006) 28–37.
[30] H. Heli, O. Amirizadeh, Non-enzymatic glucose biosensor based on hyperbranched pine-like gold nanostructure, Mater. Sci. Eng. 63 (2016) 150–154.
[31] H. Heli, S. Majdi, N. Sattarahmady, A. Parsaei, Electrocatalytic oxidation and sensitive detection of deferoxamine on nanoparticles of Fe_2O_3@ NaCo [Fe(CN)6]-modified paste electrode, J. Solid State Electrochem. 14 (2010) 1637–1647.
[32] A. Rahi, N. Sattarahmady, H. Heli, An ultrasensitive electrochemical genosensor for Brucella based on palladium nanoparticles, Anal. Biochem. 510 (2016) 11–17.
[33] N. Sattarahmady, Z. Kayani, H. Heli, Highly simple and visual colorimetric detection of Brucella melitensis genomic DNA in clinical samples based on gold nanoparticles, J. Iran. Chem. Soc. 12 (2015) 1569–1576.
[34] A. Rahi, N. Sattarahmady, R. Dehdari Vais, H. Heli, Sonoelectrodeposition of gold nanorods at a gold surface-application for electrocatalytic reduction and determination of nitrofurazone, Sens. Actuators B 210 (2015) 96–102.
[35] H. Heli, A. Jabbari, M. Zarghan, A.A. Moosavi-Movahedi, Copper nanoparticles-carbon microparticles nanocomposite for electrooxidation and sensitive detection of sotalol, Sens. Actuators B 140 (2009) 245–251.
[36] Y. Sun, Y. Xia, Shape-controlled synthesis of gold and silver nanoparticles, Science 298 (2002) 2176–2179.
[37] C. Kaittanis, S. Santra, J.M. Perez, Emerging nanotechnology-based strategies for the identification of microbial pathogenesis, Adv. Drug Deliv. Rev. 62 (2010) 408–423.
[38] K.C. Grabar, R.G. Freeman, M.B. Hommer, M.J. Natan, Preparation and characterization of Au colloid monolayers, Anal. Chem. 67 (1995) 735–743.
[39] F.R.R. Teles, L.P. Fonseca, Trends in DNA biosensors, Talanta 77 (2008) 606–623.
[40] A.A. Ali, A.B. Altemimi, N. Alhelfi, S.A. Ibrahim, Application of biosensors for detection of pathogenic food bacteria: a review, Biosensors (Basel) 10 (2020) 58.
[41] T. Endo, K. Kerman, N. Nagatani, Y. Takamura, E. Tamiya, Label-free detection of peptide nucleic acid-DNA hybridization using localized surface plasmon resonance-based optical biosensor, Anal. Chem. 77 (2005) 6976–6984.
[42] H.J. Huh, C.S. Ki, S.A. Yun, J. Lee, G.Y. Oh, N.S. Lee, Y.H. Yoon, N.Y. Lee, Comparison between DiaPlexQ™ STI6 and GeneFinder™ STD I/STD II multiplex real-time PCR kits in the detection of six sexually transmitted disease pathogens, J. Clin. Lab. Anal. 33 (2019), e22703.
[43] T. Blavo-Kouam, K.E. Angora, A. Ouattara, A. Ira-Bonouman, A.T. Offianan, J. Ouhon, H. Faye-Kett, Diagnosis of Trichomonas vaginalis using real-time polymerase chain reaction (PCR) among women at Institut Pasteur of Cte dIvoire, Afr. J. Microbiol. Res. 12 (2018) 988–993.
[44] A.M. Caliendo, J.A. Jordan, A.M. Green, J. Ingersoll, R.J. Diclemente, G. M. Wingood, Real-time PCR improves detection of Trichomonas vaginalis infection compared with culture using self-collected vaginal swabs, Infect. Dis. Obstet. Gynecol. 13 (2005) 145–150.
[45] J. Hardick, S. Yang, S. Lin, D. Duncan, C. Gaydos, Use of the Roche LightCycler instrument in a real-time PCR for Trichomonas vaginalis in urine samples from females and males, J. Clin. Microbiol. 41 (2003) 5619–5622.
[46] X.M. Hu, J.X. Xu, L.X. Jiang, L.R. Deng, Z.M. Gu, X.Y. Xie, H.C. Ji, W.H. Wang, L. M. Li, C.N. Tian, F.L. Song, Design and evaluation of a novel multiplex real-time PCR melting curve assay for the simultaneous detection of nine sexually transmitted disease pathogens in genitourinary secretions, Front. Cell. Infect. Microbiol. 9 (2019) 382.
[47] A.N. Abou Tayoun, P.R. Burchard, A.M. Caliendo, A. Scherer, G.J. Tsongalis, A multiplex PCR assay for the simultaneous detection of Chlamydia trachomatis,

Neisseria gonorrhoeae, and Trichomonas vaginalis, Exp. Mol. Pathol. 98 (2015) 214–218.

[48] S.H. Park, K.A. Hwang, J.H. Ahn, J.H. Nam, Evaluation of multiplex polymerase chain reaction assay for the simultaneous detection of sexually transmitted infections using swab specimen, J. Bacteriol. Virol. 50 (2020) 44–54.

[49] J.M. Rosenbohm, J.M. Robson, R. Singh, R. Lee, J.Y. Zhang, C.M. Klapperich, N. R. Pollock, M. Cabodi, Rapid electrostatic DNA enrichment for sensitive detection of Trichomonas vaginalis in clinical urinary samples, Anal. Methods 12 (2020) 1085–1093.